Spectroscopic and Excited-State Properties of Tri-9-anthrylborane I: Solvent Polarity Effects

Noboru Kitamura* and Eri Sakuda

Division of Chemistry, Graduate School of Science, Hokkaido University, 060-0810 Sapporo, Japan

Received: February 8, 2005; In Final Form: June 22, 2005

Spectroscopic and excited-state properties of tri-9-anthrylborane (**TAB**), showing unique absorption and fluorescence characteristics originating from p(boron)−π(anthryl group) orbital interactions, were studied in 12 solvents. Although the absorption maximum energy (ν_a) of **TAB** which appeared at around 21×10^3 cm^{-1} (band I) was almost independent of the solvent polarity parameter, $f(X)$ ($f(X) = (D_s - 1)/(2D_s + 1) - (n^2 - 1)/(2n^2 + 1)$ where D_s and n represent the static dielectric constant and the refractive index of a solvent, respectively), the fluorescence maximum energy (ν_f) showed a linear correlation with $f(X)$. The $f(X)$ dependence of the value of $\nu_a - \nu_f$ demonstrated that the change in the dipole moment of **TAB** upon light excitation was ∼8.0 D, indicating that absorption band I was ascribed to an intramolecular charge-transfer transition in nature. The excited electron of **TAB** was thus concluded to localize primarily on the p orbital of the boron atom. Furthermore, it was shown that the fluorescence lifetime and quantum yield of **TAB** varied from 11.8 to 1.1 ns and from 0.41 to 0.02, respectively, with an increase in $f(X)$. The present results indicated that the nonradiative decay rate constant (k_{nr}) of **TAB** was influenced significantly by $f(X)$. Excited-state decay of **TAB** was understood by intramolecular back-electron (charge) transfer from the p orbital of the boron atom to the π orbital of the anthryl group, which was discussed in terms of the energy gap dependence of k_{nr}. Specific solvent interactions of **TAB** revealed by the present spectroscopic and photophysical studies are also discussed.

Introduction

Boron-containing π-conjugated systems, including their polymers, are a subject of current interest because of their unique optical and electrochemical properties,[1−8] and their derivatives are expected to play important roles in optoelectronic and LED devices.[9,10] In particular, boron systems with relatively large π-electron chromophores show quite interesting spectroscopic and photophysical properties.[11−15] As an example, Yamaguchi et al. have reported that tri-9-anthrylborane (**TAB**, see Scheme 1) in tetrahydrofuran (THF) exhibits a broad and intense absorption band at around 470 nm (band I), in addition to a structured anthracene-like band (band II) in the wavelength region of 330−380 nm at room temperature.[11] The compound also shows broad and structureless fluorescence in 480−650 nm. Because dilute solutions of anthracene and its derivatives are well-known to show structured absorption and fluorescence spectra at around 330−380 and 380−480 nm, respectively,[16] the appearance of the absorption band I and the red-shifted fluorescence of **TAB** are very interesting. According to the theoretical calculations by Yamaguchi et al., the HOMO and second HOMO (HOMO-1) of **TAB** degenerate with each other and are respectively localized primarily on one anthryl group with the significant density being distributed on the adjacent anthryl group, while the LUMO is delocalized over three anthryl groups via the p orbital of the boron atom (Figure 3 in ref 11). On the basis of such calculations, they concluded that band I, observed for **TAB**, was attributed to the HOMO−LUMO and HOMO-1−LUMO transitions.[11]

Analogous aryl-substituted main group elements (Si and P) also exhibit very interesting absorption and fluorescence characteristics similar to **TAB**.[17,18] Although the photophysics of organosilane compounds have been studied extensively,[19] the number of studies on the photophysics of boron-containing π-electron systems is still limited, except for the reports by Yamaguchi et al.[11−15] In particular, a systematic study on the excited-state properties of the compound such as a fluorescence lifetime, radiative and nonradiative rate constants, and so forth has not been explored until now. It is worth noting that the spectroscopic properties of triarylboranes have been reported by Ramsey[20] and another research group.[21] Ramsey demonstrated that, since the lower energy shift of the absorption band of triarylborane by a variation of the π-electron chromophore (aryl = phenyl, tolyl, mesityl, or naphthyl group) correlated linearly with the decreasing order of the ionization potential of the aryl group, the absorption band observed for the compound could be assigned to an intramolecular charge-transfer (CT) transition.[20]

SCHEME 1: Structure of Tri-9-anthrylborane (TAB)

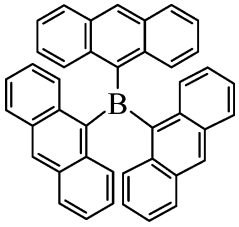

In the course of studying boron-containing π-chromophore systems, we found that the spectroscopic and excited-state properties of **TAB**, as a reference compound for our study, showed marked solvent dependences. Furthermore, the fluorescence lifetime and quantum yield of **TAB** were also strongly dependent on the solvent. Our experimental observations raised

* To whom all correspondence should be addressed. E-mail: kitamura@sci.hokudai.ac.jp.

10.1021/jp0507039 CCC: $30.25
Published on Web 07/30/2005

the simple question of whether or not the delocalized LUMO reported by Yamaguchi et al. explains the solvent effects on the spectroscopic and excited-state characteristics of **TAB**. Furthermore, the spectroscopic properties of triarylboranes reported by Ramsey are also worth comparing with those of **TAB**. To obtain basic understanding of the photophysical properties of boron-containing π-electron systems, we studied solvent effects on the spectroscopic/excited-state properties and electroabsorption/electrofluorescence spectra of **TAB** in polymer films.

In this paper, we report solvent effects on the spectroscopic and excited-state properties of **TAB** in 12 solvents. Solvent effects on the absorption and fluorescence characteristics of **TAB** demonstrated that the excited-electron of **TAB** was localized on the p orbital of the boron atom [abbreviated as p(B)] and, thus, the lowest electronic transition was best described by electron (charge) transfer between the π orbital of the anthryl group [abbreviated as π(An)] and p(B). The results were discussed in terms of those obtained by electroabsorption/electrofluorescence spectroscopy (i.e., Stark spectroscopy) of **TAB**, reported in the next paper in this issue (Part II of the series).[22] These results also indicate that nonradiative decay from the excited state of **TAB** should be explained by intramolecular back-electron (charge) transfer from p(B) to π(An). The large solvent dependence of the nonradiative decay rate constant of **TAB** was then discussed in terms of the energy gap law, similar to that reported for the metal-to-ligand charge-transfer excited state of $Ru(bpy)_3^{2+}$ or $Os(bpy)_3^{2+}$ (bpy = 2,2′-bipyridine).[23]

Experimental Section

Chemicals. Tri-9-anthrylborane (**TAB**) was synthesized according to the literature[11] and purified successively by column chromatography on alumina (chloroform/*n*-hexane = 1:1 vol %) and repeated recrystallizations from benzene. The structure and purity of **TAB** were confirmed by ^{1}H NMR and elemental analysis.[24] Spectroscopic grade solvents were obtained from Wako Pure Chemicals Co. Ltd. and purified by accepted procedures, if necessary.[25]

Measurements. Steady-state absorption spectroscopy was conducted with a Hitachi U-3300 spectrophotometer, and corrected fluorescence spectra were recorded on a Hitachi F-4500 spectrofluorometer. The fluorescence quantum yield (Φ_f) of **TAB** was determined using Rhodamin B as a standard (Φ_f = 0.65 in ethanol).[26] The absorbance of a sample solution at an excitation wavelength (385 nm) was set 0.05 and refractive index correction was made to determine Φ_f in each solvent. Fluorescence decay measurements were conducted using a picosecond single-photon counting system.[27] Knowing Φ_f and the fluorescence lifetime of **TAB** (τ_f) in each solvent, we determined the radiative (k_f) and nonradiative rate constants of **TAB** (k_{nr}) according to the relationship $\Phi_f = k_f/(k_f + k_{nr}) = k_f \tau_f$. For fluorescence spectroscopy, sample solutions were deaerated by purging with an Ar gas stream for 20 min.

Results

Absorption and fluorescence spectra of **TAB** in several solvents are shown in Figures 1 and 2, respectively. In THF, **TAB** showed a relatively broad absorption band at a maximum energy (ν_a) of 21.1 × 10^3 cm^{-1} (band I) in addition to a structured anthracene-like absorption at (25−30) × 10^3 cm^{-1} (band II). On the other hand, the compound exhibited broad and structureless fluorescence at a maximum energy (ν_f) of 18.7 × 10^3 cm^{-1}. The absorption/fluorescence spectral band shapes

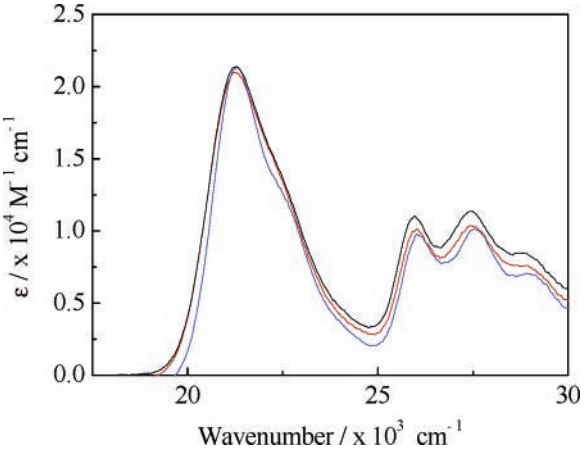

Figure 1. Absorption spectra of **TAB** in THF (black), cyclohexane (blue), and acetonitrile (red).

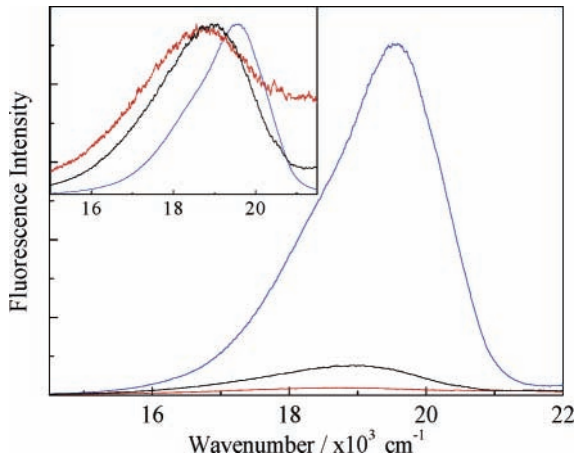

Figure 2. Fluorescence spectra of **TAB** in THF (black), cyclohexane (blue), and acetonitrile (red). The inset is the spectra normalized to the maximum intensity.

and their maximum energies in THF agreed very well with those reported by Yamaguchi et al, including a weak fluorescence shoulder at around ∼18 × 10^3 cm^{-1} (∼560 nm).[11] The absorption and fluorescence parameters determined in 12 solvents are summarized in Table 1: ν_a, the molar absorptivity (ϵ), ν_f, and the full-width at half-maximum (fwhm) of the absorption or fluorescence spectrum. It is worth noting that the broad fluorescence band of **TAB**, different from monomer fluorescence of anthracene itself, is not caused by an intermolecular interaction between **TAB** moelcules because these experiments were conducted in the concentration range of ∼10^{-6} M. Furthermore, the fluorescence is not explained by intramolecular excimer formation between the anthryl groups because two of any π planes in **TAB** do not take a parallel orientation as predicted from the X-ray structure of the molecule.[11] Therefore, both absorption band I and the fluorescence of **TAB** are caused by the participation of p(B)−π(An) interactions, as discussed in the following sections.

Figure 3 shows the fluorescence decay profiles of **TAB** in several solvents (monitored at the peak energy in each solvent). Since the decay profile was fitted satisfactorily by a single exponential function regardless of the solvent, the excited-state lifetime (τ_f) of **TAB** and thus k_f and k_{nr} could be determined accurately. The excited-state parameters of **TAB** (Φ_f, τ_f, k_f, and k_{nr}) determined in each solvent are summarized in Table 2.

The present observations demonstrated that the ν_a of absorption band I (∼21 × 10^3 cm^{-1}) or band II (∼26 × 10^3 cm^{-1}, the

TABLE 1: Spectroscopic Properties of TAB at 25 °C

		absorption			fluorescence		solvent parameters[a]			
no.	solvent	ν_a $\times 10^3$ cm^{-1}	ϵ (log ϵ) $\times 10^4$ M^{-1} cm^{-1}	fwhm cm^{-1}	ν_f $\times 10^3$ cm^{-1}	fwhm cm^{-1}	$f(X)$	D_s	n	η cP
1	cyclohexane	21.3	2.11 (4.32)	2260	19.5	2270	−0.001	2.02	1.423	0.898
2	toluene	21.1	2.31 (4.36)	2410	19.2	2170	0.013	2.38	1.494	0.552
3	propionic acid	21.3	1.66 (4.22)	2430	19.1	2400	0.119	3.44	1.384	0.958
4	chloroform	21.2	2.12 (4.33)	2460	18.9	2470	0.147	4.81	1.443	0.514
5	ethyl acetate	21.3	1.84 (4.27)	2450	19.0	2660	0.200	6.02	1.370	0.426
6	tetrahydrofuran	21.2	2.14 (4.33)	2480	18.7	2980	0.210	7.58	1.405	0.460
7	dichloromethane	21.2	1.94 (4.29)	2370	18.7	2790	0.217	8.93	1.421	0.393
8	1,2-dichloroethane	21.2	1.86 (4.27)	2590	18.6	3140	0.221	10.4	1.442	0.730
9	1-butanol	21.3	1.12 (4.05)	2450	18.9	2820	0.264	17.5	1.397	2.271
10	acetone	21.3	2.06 (4.32)	2500	18.6	2750	0.284	20.7	1.356	0.304
11	ethanol	21.3	1.01 (4.00)	2570	18.9	3200	0.289	24.6	1.359	1.078
12	acetonitrile	21.3	2.10 (4.32)	2460	18.6	3370	0.305	37.5	1.342	0.325

[a] Data taken from ref 28.

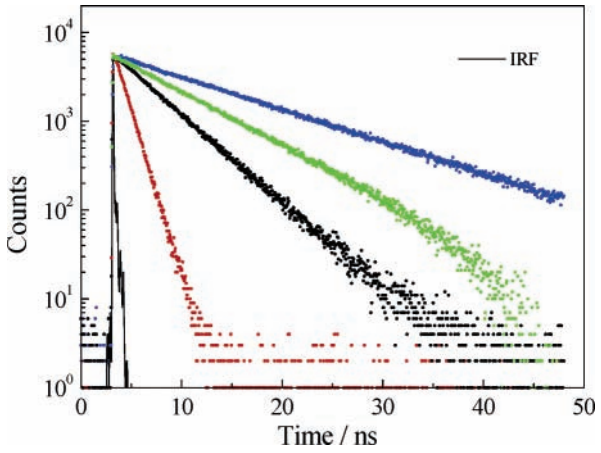

Figure 3. Fluorescence decay profiles of **TAB** in cyclohexane (blue), toluene (green), THF (black), and acetonitrile (red). IRF represents the instrumental response.

TABLE 2: Excited-State Properties of TAB at 25 °C

no.	solvent	Φ_f	τ_f ns	k_f $\times 10^7$ s^{-1}	k_{nr} (ln k_{nr}) $\times 10^8$ s^{-1}
1	cyclohexane	0.41	11.8	3.5	0.5 (17.7)
2	toluene	0.17	7.2	2.4	1.2 (18.6)
3	propionic acid	0.09	4.3	2.1	2.1 (19.1)
4	chloroform	0.05	3.2	1.6	3.0 (19.5)
5	ethyl acetate	0.07	3.5	2.0	2.7 (19.4)
6	tetrahydrofuran	0.06	4.3	1.4	2.2 (19.2)
7	dichloromethane	0.02	2.3	0.9	4.2 (19.9)
8	1,2-dichloroethane	0.03	1.8	1.7	5.5 (20.1)
9	1-butanol	0.04	2.0	2.0	4.8 (20.0)
10	acetone	0.02	1.6	1.2	6.0 (20.2)
11	ethanol	0.05	1.6	3.1	5.8 (20.2)
12	acetonitrile	0.02	1.1	1.8	8.7 (20.6)

data are not shown here) was almost independent of solvent, while the ϵ and fwhm values of each absorption band varied marginally with a medium, except for the relatively small ϵ value in 1-butanol or ethanol as compared to those in other solvents. On the other hand, the ν_f and fwhm values of the fluorescence spectrum were influenced significantly by the solvent (Table 1 and Figure 2). As a typical example, a variation of the medium from cyclohexane to CH_3CN resulted in a change in ν_f (fwhm) from 19.5 $\times$ 10^3 (2270) to 18.6 $\times$ 10^3 cm^{-1} (3370 cm^{-1}). Furthermore, the large solvent effects on the fluorescence spectrum accompanied those on Φ_f and τ_f. Namely, the lower-energy shift of the fluorescence spectrum on changing from cyclohexane to CH_3CN resulted in large decreases in both Φ_f (0.41−0.02) and τ_f (11.8−1.1 ns).

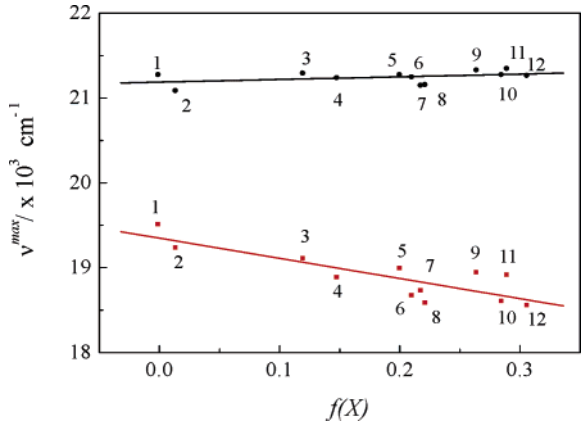

Figure 4. Solvent polarity parameter [$f(X)$] dependences of the absorption (ν_a shown in black) and fluorescence maximum energies (ν_f shown in red). The numbers inserted in the figure correspond to those in Table 1.

Table 1 includes the following representative solvent properties: static dielectric constant (D_s), refractive index (n), and viscosity (η).[28] It is clear from Tables 1 and 2 that the solvent dependences of the spectroscopic and excited-state properties of **TAB** are correlated well with the solvent polarity parameter (D_s or n), but not with η. In the following sections, therefore, we focus our discussion on the solvent polarity dependences of the observed data.

Discussion

Solvent Polarity Dependences of the Absorption and Fluorescence Spectra. It is well-known that solvent polarity effects on the spectroscopic properties of a molecule are described by contributions from D_s and n of a solvent, where D_s and n (n^2, is the optical dielectric constant) are related to dipole orientation and electronic polarizability of a solvent molecule, respectively.[29] To discuss such contributions, the following solvent polarity parameter, $f(X)$, is in general employed, eq 1[29]

$$f(X) = \frac{D_s - 1}{2D_s + 1} + \frac{n^2 - 1}{2n^2 + 1} \quad (1)$$

Figure 4 shows the $f(X)$ dependences of ν_a (band I) and ν_f, where the numbers indicated in the figure correspond to those in Table 1. As described in the previous section, it is clear that ν_a (shown by black) is almost independent of $f(X)$. Although the data were not shown here, the ν_a of band II was also insensitive to $f(X)$.

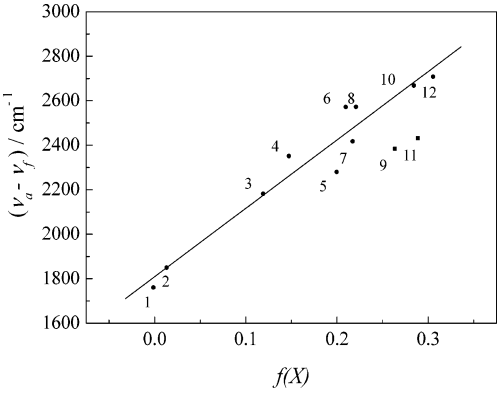

Figure 5. Solvent polarity parameter [$f(X)$] dependence of the Stokes shift ($\nu_a - \nu_f$). The numbers inserted in the figure correspond to those in Table 1.

On the other hand, Table 1 demonstrates that the ϵ value is dependent on a solvent [$(1.01-2.31) \times 10^4$ M^{-1} cm^{-1}]. In particular, the values in 1-butanol (1.12×10^4 M^{-1} cm^{-1}) and ethanol (1.01×10^4 M^{-1} cm^{-1}) were very small compared to those in other solvents, and the value in propionic acid (1.66×10^4 M^{-1} cm^{-1}) was also somewhat smaller than those in the aprotic solvents. Such a large variation of ϵ with $f(X)$ suggests HOMO−LUMO overlap in **TAB**. It has been reported that the extent of the HOMO−LUMO overlap is dependent on the degree of steric hindrance in triarylborane; the ϵ values of triphenylborane and trimesitylborane are 3.6×10^4 and 1.6×10^4 M^{-1} cm^{-1}, respectively; the value is smaller for the compound with bulkier aryl groups.[20] Although the fwhm of the spectrum also varied slightly with a solvent (2260−2570 cm^{-1}), we could not confirm one-to-one correspondence between the variations in ϵ and fwhm. Organoborane derivatives are, in general, unstable in a protic solvent and water, suggesting direct interactions of the solvent with p(B). The very small ϵ values in 1-butanol and ethanol as compared to those in other solvents would therefore be the result of specific interactions of the alcohol (and propionic acid) with **TAB**. In the other nine solvents, the marginal $f(X)$ dependence of ϵ can be attributed to the variation of the conformation of **TAB** (i.e., the extent of the HOMO−LUMO overlap (discussed later).

Figure 4 demonstrates that the ν_f value (shown in red) decreases with an increase in $f(X)$: the slope value $= -2850$ cm^{-1} and the correlation coefficient (r) $= 0.72$ for 12 solvents. The slope of the plot suggests that the radiative process of **TAB** accompanies a relatively large dipole moment change. It is well-known that the electric dipole moment change upon an electronic transition, $\Delta\mu$ ($= \mu_g - \mu_e$, where μ_g and μ_e represent the dipole moments of a molecule in the ground and excited states, respectively), can be estimated on the basis of the data in Figure 4 and the following equation[30−32]

$$(\nu_a - \nu_f) \cong \frac{2\Delta\mu^2}{hca^3} f(X) + A \qquad (2)$$

where h, c, a, and A represent the Planck's constant, the speed of light, the radius of **TAB** (Onsager radius, assumed to be 9.0 Å), and a constant, respectively. As can be seen from the data shown in Figure 5, we obtained a good linear relationship between $\nu_a - \nu_f$ and $f(X)$, with the data in 1-butanol and ethanol (nos. 9 and 11) being deviated from the linear relationship. For the calculation of the slope of the plot, we omitted these data because specific interactions between **TAB** and the alcohols were suggested as described before. The slope value was then

SCHEME 2: Structure of a Dibenzoborole-Containing π-Electron System (DB), where Ar Represents an Aromatic or Heteroaromatic Ring

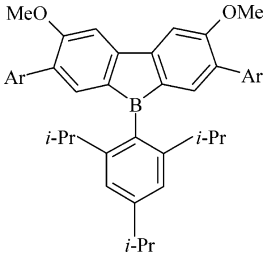

calculated to be 3070 cm^{-1} ($r = 0.97$), and this gave a $\Delta\mu$ value of ∼8.0 D. Because ν_a is almost independent of $f(X)$, μ_e should be responsible for large $\Delta\mu$ ($\mu_e \approx \Delta\mu$). As described in detail in Part II of this series,[22] Stark spectroscopy provides direct information about $\Delta\mu$. The $\Delta\mu$ value determined for **TAB** by Stark spectroscopy was 7.8 D, which agreed very well with the present observation. Therefore, we conclude that $\Delta\mu$ of **TAB** is 7.8−8.0 D. It is worth emphasizing that the $\Delta\mu$ value of **TAB** is as large as that of an intramolecular charge-transfer-type compound. As an example, $\Delta\mu$ of 4-amino-4′-nitrobiphenyl has been reported to be 12 D.[30,32] Although the large $\Delta\mu$ value of 4-amino-4′-nitrobiphenyl can be readily understood because of the presence of the donor and acceptor groups along the long axis of a biphenyl backbone, that of structurally symmetrical **TAB** is extraordinary.

Solvent effects on the fluorescence spectrum of a boron-containing π-conjugated system have been already reported.[12,15] In particular, it has been demonstrated that dibenzoborole-containing π-electron systems (**DB,** see Scheme 2) show large solvent effects on the fluorescence spectrum.[15] The **DB** derivatives display fluorescence maxima at around 560−580 nm in THF, while the spectrum shifts to the shorter wavelength (420−480 nm) in a donor solvent such as CH_3CN, *N*,*N*-dimethylformamide, or *N*,*N*-dimethylacetamide. The results were explained by coordination of the donor solvent to p(B), which prevented delocalization of the electron in the LUMO (blue shift of the spectrum). In the excited state of **TAB**, we suppose that a solvent molecule interacts more or less with p(B). Nevertheless, the ν_f value of **TAB** showed the lower-energy shift with a variation of the solvent from THF to CH_3CN, which was opposite to the solvent shift observed for **DB**. Although we are not certain about the differences in the solvent shift of the fluorescence spectrum between **TAB** and **DB**, one possible explanation might be the crowding around p(B); it is more crowded for **TAB** which prevents direct and strong coordination of a solvent molecule to p(B) (see Schemes 1 and 2). The above discussions indicate that, although the solvent effects on the fluorescence characteristics of **DB** are very specific, the linear relationship in Figure 5, except for the data in 1-butanol and ethanol, indicates that the spectroscopic properties of **TAB** should be discussed as common solvent effects without specific solute−solvent interactions (see the next section).

It is worth pointing out that the $\Delta\mu$ value of **TAB** (7.8−8.0 D) indicates that the excited state is not explained by the delocalized LUMO.[11] If the LUMO is delocalized over **TAB** via p(B), such a large $\Delta\mu$ would not be expected because of the symmetrical structure of the compound. The present results indicate, therefore, that the excited state of **TAB** is localized on p(B). In practice, our theoretical considerations indicated that the lowest-singlet excited state of **TAB** was charge transfer (CT) in origin and the amount of the charge transferred (q) from π(An) to p(B) was estimated to be as large as $q \approx 1.0$.[22] These

theoretical considerations agree satisfactorily with the experimental results in Figure 5 as well as with the electroabsorption/electrofluorescence spectra of **TAB** (i.e., $\Delta\mu = 7.8$ D).[22] Absorption band I and the fluorescence observed for **TAB** are thus essentially attributed to the CT transition. The results also agree with the old works by Ramsey and another research group.[20,21]

On the other hand, it has been reported that anthryldimesitylborane (An(mes)$_2$B, two anthryl groups in **TAB** are replaced by mesityl groups) in THF shows a ν_a much higher in energy (23.8×10^3 cm^{-1}, 420 nm) than that of **TAB** (21.2×10^3 cm^{-1}, 470 nm).[13] Our preliminary experiments on the effects of the solvent on the absorption and fluorescence spectra of An(mes)$_2$B indicated that the μ_e value of the molecule was ~7.0 D, which was comparable to that of **TAB**. Therefore, we think that the LUMO of An(mes)$_2$B is also localized on p(B), as in **TAB**. However, the lower ν_a value of **TAB**, compared to that of An(mes)$_2$B, suggests an electronic interaction between the anthryl groups in **TAB**. When one assumes that the oxidation (E_p^{ox}) and reduction potentials (E_p^{red}) of a molecule correspond to the HOMO and LUMO energies, respectively, the HOMO−LUMO energy gap ($\Delta E = E_p^{ox} - E_p^{red}$) of **TAB** or An(mes)$_2$B is calculated to be $\Delta E = 2.70$ or 2.92 V, respectively: $E_p^{ox} = 1.36$ and $E_p^{red} = -1.34$ V for **TAB** and $E_p^{ox} = 1.30$ and $E_p^{red} = -1.62$ V for An(mes)$_2$B (vs SCE in *N*,*N*-dimethylformamide, 0.1 M *n*-Bu$_4$NPF$_6$).[33] The ΔE values agree very well with the ν_a values of **TAB** (21.2×10^3 cm^{-1} = 2.63 eV) and An(mes)$_2$B (23.8×10^3 cm^{-1} = 2.95 eV). Since the behavior is very similar to the metal-to-ligand charge-transfer (MLCT) transition in polypyridine Ru^{2+} complexes,[34,35] the results also support electron transfer from π(An) to p(B) in the excited state of **TAB** or An(mes)$_2$B. However, because the E_p^{ox} value of **TAB** is almost comparable with that of An(mes)$_2$B, the difference in ν_a and, thus ΔE, between the two compounds is responsible for that in E_p^{red} (LUMO energy). Therefore, the electronic interactions, excited-state energy hopping (i.e., hole hopping), or both between the anthryl groups would also play a role, partly, in determining the LUMO energy of **TAB**. Although further theoretical studies are needed to reveal the explicit origins of the HOMO and LUMO of **TAB**, the present experiments indicate that the excited state of **TAB** is best described by the localized LUMO, while the electronic interactions between the anthryl groups contribute to the excited state to some extent.

Solvent Polarity Dependences of the Excited-State Properties. With an increase in $f(X)$ from −0.001 (cyclohexane) to 0.305 (CH$_3$CN), the Φ_f or τ_f value decreased by a factor of ~20 (0.41−0.02) or ~10 (11.8−1.1 ns), respectively (Table 2). Such large solvent dependences of the excited-state properties will be very characteristic to **TAB** with the excited state being localized on p(B) with $q \approx 1.0$. A close inspection of Table 2 indicates that the k_f value is in the range of $(0.9-3.5) \times 10^7$ s^{-1}, while k_{nr} varies from 0.5×10^8 to 8.7×10^8 s^{-1} with $f(X)$. Thus, the major influence of $f(X)$ on the excited state of **TAB** is that on k_{nr}. The above discussions indicate that nonradiative decay from the excited state of **TAB** is associated with intramolecular back-electron transfer from p(B) to π(An). This situation is very similar to nonradiative decay from the MLCT excited state of Ru(bpy)$_3^{2+}$ or Os(bpy)$_3^{2+}$, in which nonradiative decay is associated with back-electron transfer from the π^* orbital of the ligand to the metal t_{2g} orbital.[36] So far, the solvent effects on the k_{nr} of Ru(bpy)$_3^{2+}$ have been discussed in terms of the energy gap law by Meyer and co-workers; ln k_{nr} was shown to be correlated linearly with the energy gap between the ground and excited states of the complex (E_{em}).[23]

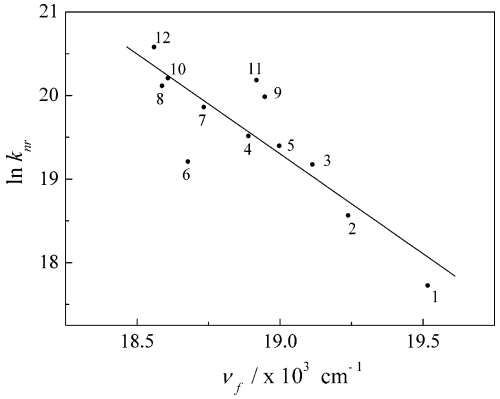

Figure 6. Energy gap (ν_f) dependence of ln k_{nr}. The numbers inserted in the figure correspond to those in Table 1.

The essence of the energy gap dependence of ln k_{nr} is given by eq 3[23]

$$\ln k_{nr} \propto -\frac{\gamma_0 E_{em}}{\hbar\omega} \tag{3}$$

where ω is the angular frequency of the vibration(s) responsible for nonradiative decay and γ_0 is given by

$$\gamma_0 = \ln \frac{E_{em}}{S\hbar\omega} - 1 \tag{4}$$

where S is the parameter related to the vibrational displacement between the ground and excited states. Although the E_{em} term is included in γ_0, this contribution to an energy gap plot has been reported to be minor.[23] Therefore, ln k_{nr} should correlate linearly with E_{em} under the assumptions of the energy gap law.

In the present experiments, since ν_a is almost independent of $f(X)$, the ν_f value as a measure of E_{em} in a given medium was plotted against the relevant ln k_{nr} value (Figure 6). As can be seen in the figure, we obtained a linear relationship between ln k_{nr} and ν_f for 9 solvents, except for the data in THF, 1-butanol, and ethanol (nos. 6, 9, and 11): slope = -2.7×10^{-3} cm^{-1} ($r = 0.98$). The deviation of the data in 1-butanol and ethanol from the linear relationship will be explained by the specific solute−solvent interactions as discussed before. The larger k_{nr} values in the alcohols than those predicted from the relevant ν_f value indicate that nonradiative decay from **TAB** takes place more efficiently in a protic solvent. Such effects of a protic solvent on nonradiative decay have been also reported for the MLCT excited states of Ru(bpy)$_3^{2+}$ and related complexes, and the results have been explained by contributions of the high-frequency O−H vibrations of the medium to excited-state decay.[37−39] Since **TAB** is likely to interact with a protic solvent through p(B), the present results would be also explained by such solute−solvent interactions. Furthermore, the value in THF also deviated, unexpectedly, from the linear relationship, and nonradiative decay was impeded considerably, as expected from the ν_f value. Because the electron is localized on p(B) in the excited state of **TAB**, the lone-pair electrons of the oxygen atom in THF might be repelled from p(B). Although there is no direct evidence, such a situation might make nonradiative decay less efficient as compared to that in other aprotic solvents with similar $f(X)$ values.

On the other hand, the linear relationship between ln k_{nr} and ν_f in the 9 solvents indicates that the variation of the solvent does not bring about large changes in the electronic structures, deactivation mode, or both of **TAB**. Since the excited electron of **TAB** is localized on p(B), the solvent orientation around the

excited state [i.e., with an increase in $f(X)$] decreases its energy resulting in the energy gap dependence of ln k_{nr}. It may be worth noting that the slope of the plot for **TAB** (-2.7×10^{-3} cm^{-1}) is much steeper than that for the solvent effects on Ru(bpy)$_3^{2+}$ (-9.3×10^{-4} cm^{-1}).[23] Since the deactivation mode of the excited state, related to ω in eq 3, is totally different between the two systems, a direct comparison of the values is impossible. In the case of Ru(bpy)$_3^{2+}$, however, it has been reported that nonradiative decay is induced by the breathing vibrations of the 2,2-bipyridine ligand ($\hbar\omega = 1300-1400$ cm^{-1}).[23,38,39] To explain the large solvent dependence of the ln k_{nr} values of **TAB** in Figure 6, eq 3 indicates that nonradiative decay of **TAB** should involve very low-frequency vibrations. However, **TAB** showed no important low-frequency vibration as demonstrated by the IR spectrum, and the frequency of the Raman active boron−carbon stretching vibration has been reported to be 1250−1280 cm^{-1},[40] which is comparable to the breathing vibration of 2,2′-bipyridine. At the present stage of the investigation, therefore, we suppose that ω will not be the primary reason for the large slope value in Figure 6.

Another factor determining the slope of the plot is γ_0. The linear relationship between ln k_{nr} and ν_f indicates that γ_0 also varies linearly with ν_f and that the variation of γ_0 with ν_f should be governed by S. As described in the preceding section, the ϵ value varies with $f(X)$ [$(1.84-2.31) \times 10^4$ M^{-1} cm^{-1} except for those in 1-butanol and ethanol], and the results would be explained in terms of the variation of the extent of the HOMO−LUMO overlap, probably caused by that of the conformation of **TAB** with a solvent. This will more or less induce the change in S because S is related to the extent of the distortion in the excited state for those vibrations contributing to excited-state decay.[38,39] A smaller electron−vibrational coupling strength for **TAB** as compared to that for Ru(bpy)$_3^{2+}$ would account for the larger slope in Figure 6. Clearly, more detailed studies, including resonance Raman spectroscopy and Franck−Condon analysis of the fluorescence spectrum of **TAB**, are absolutely necessary to explicitly explain the present results. Nonetheless, the energy gap analysis of the k_{nr} data revealed the characteristics of the solvent effects on the excited-state properties of **TAB**.

Conclusions

The present study revealed the spectroscopic and excited-state properties of **TAB** in detail. The large $f(X)$ dependence of the fluorescence characteristics (ν_f, τ_f, and Φ_f) demonstrated that the excited electron in **TAB** was localized on p(B). The results were supported by the $f(X)$ dependence of the Stokes shift ($\Delta\mu \approx 8.0$ D) as well as by Stark spectroscopy ($\Delta\mu = 7.8$ D) reported in the next paper in this issue.[22] The absorption band at $\nu_a \approx 2.1 \times 10^{-3}$ cm^{-1} was thus concluded to be the electronic transition from the π orbital of the anthryl group to the vacant p orbital of the boron atom. This demonstrates that the nonradiative decay from the excited state of **TAB** involves intramolecular back-electron transfer from p(B) to π(An). Therefore, the vacant p orbital on the boron atom in **TAB** plays an essential role in determining the spectroscopic and excited-state properties of the compound. Boron-containing π-conjugated systems other than **TAB** also exhibit quite interesting spectroscopic properties,[11−15] which are worth studying in more detail. Further studies on the photophysical properties of several boron-containing π-conjugated systems are now in progress in our laboratory, which will reveal characteristics of the ground and excited states of the systems.

Acknowledgment. The authors are indebted to Prof. N. Ohta, Dr. T. Iimori, and Mr. T. Yoshizawa at the Research Institute for Electronic Science, Hokkaido University, for their invaluable discussions and to one of the reviewers for the valuable comments on the energy gap analysis of the present data. N.K. also acknowledges a grant-in-aid for Scientific Research from the Ministry of Education, Culture, Sports, Science and Technology (MEXT) of the Japanese Government for the support of the research (Nos. 138530004 and 14050001).

References and Notes

(1) Yuan, Z.; Taylor, N. J.; Marder, T. B.; Williams, I. D.; Kurtz, S. K.; Cheng, L.-T. *J. Chem. Soc., Chem. Commun.* **1990**, 1489.
(2) Yuan, Z.; Taylor, N. J.; Sun, Y.; Marder, T. B.; Williams, I. D.; Cheng, L.-T. *J. Orgnomet. Chem.* **1993**, *449*, 27.
(3) Yuan, Z.; Taylor, N. J.; Ramachandran, R.; Marder, T. B. *Appl. Organomet. Chem.* **1996**, *10*, 305.
(4) Yuan, Z.; Collings, J. C.; Taylor, N. J.; Marder, T. B.; Jardin, C.; Halet, J. F. *J. Solid State Chem.* **2000**, *154*, 5.
(5) Lee, B. Y.; Wang, S.; Putzer, M.; Bartholomew, G. P.; Bu, X.; Bazan, G. C. *J. Am. Chem. Soc.* **2000**, *122*, 3969.
(6) Lee, B. Y.; Bazan, G. C. *J. Am. Chem. Soc.* **2000**, *122*, 8577.
(7) Matsumi, N.; Naka, K.; Chujo, Y. *J. Am. Chem. Soc.* **1998**, *120*, 5112.
(8) Matsumi, N.; Naka, K.; Chujo, Y. *J. Am. Chem. Soc.* **1998**, *120*, 10776.
(9) Noda, T.; Shirota, Y. *J. Am. Chem. Soc.* **1998**, *120*, 9714.
(10) Noda, T.; Ogawa, H.; Shirota, Y. *Adv. Mater.* **1999**, *11*, 283.
(11) Yamaguchi, S.; Akiyama, S.; Tamao, K. *J. Am. Chem. Soc.* **2000**, *122*, 6335.
(12) Yamaguchi, S.; Shirasaka, T.; Tamao, K. *Org. Lett.* **2000**, *2*, 4129.
(13) Yamaguchi, S.; Akiyama, S.; Tamao, K. *J. Am. Chem. Soc.* **2001**, *123*, 11372.
(14) Yamaguchi, S.; Akiyama, S.; Tamao, K. *J. Orgnomet. Chem.* **2002**, *652*, 3.
(15) Yamaguchi, S.; Shirasaka, T.; Akiyama, S.; Tamao, K. *J. Am. Chem. Soc.* **2002**, *124*, 8816.
(16) Birks, J. B. *Photophysics of Aromatic Hydrocarbons*; Wiley-Interscience: London, 1970.
(17) Yamaguchi, S.; Akiyama, S.; Tamao, K. *Organometallics* **1998**, *17*, 4347.
(18) Yamaguchi, S.; Akiyama, S.; Tamao, K. *J. Am. Chem. Soc.* **2000**, *122*, 6793.
(19) For example, see: Yamamoto, M.; Kudo, T.; Ishikawa, M.; Tobita, S.; Shizuka, H. *J. Phys. Chem. A* **1999**, *103*, 3144.
(20) Ramsey, B. G. *J. Phys. Chem.* **1966**, *70*, 611.
(21) Miller, D. S.; Leffler, J. E. *J. Phys. Chem.* **1970**, *74*, 2571.
(22) Part II of this series: Kitamura, N.; Sakuda, E.; Yoshizawa, T.: Iimori, T.; Ohta, N. *J. Phys. Chem.* **2005**, *109*, 7435.
(23) Casper, J. V.; Meyer, T. J. *J. Am. Chem. Soc.* **1983**, *105*, 5583.
(24) ^{1}H NMR ($CDCl_3$, 300 MHz): δ 8.55 (s, 3H), 8.05 (d, 6H), 7.97 (d, 6H), 7.27 (m, 6H), 6.90 (m, 9H). Elemental analysis $C_{42}H_{27}B$, calcd (found): C, 92.99 (92.83); H, 5.02 (5.23).
(25) Perrin, D. D.; Armarego, W. L. F.; Perrin, D. R. *Purification of Laboratory Chemicals*, 2nd ed.; Pergamon Press: New York, 1980.
(26) Murov, S. L.; Carmichael, I.; Hug, G. L. *Handbook of Photochemistry*; Marcel Dekker: New York, 1993.
(27) Kim, H.-B.; Habuchi, S.; Kitamura, N. *Anal. Chem.* **1999**, *71*, 842.
(28) *Organic Solvent*, 3rd ed; Riddick, J. A., Bunger, W. B., Eds.; Techniques of Chemistry, Vol. II; Wiley-Interscience: New York, 1970.
(29) Suppan, P.; Ghoneim, N. *Solvatochromism*; The Royal Society of Chemistry: Cambridge, **1997**.
(30) Lippert, E. *Z. Naturforsch.* **1955**, *10a*, 541.
(31) Mataga, N.; Kaifu, Y.; Koizumi, M. *Bull. Chem. Soc. Jpn.* **1955**, *28*, 69.
(32) Mataga, N.; Kubota, T. *Molecular Interactions and Electronic Spectra*; Marcel Dekker: New York, **1970**.
(33) Both derivatives showed irreversible redox waves, so that the data were shown as the peak values. The reduction potentials of **TAB** and An(mes)$_2$B have been also reported by Yamaguchi et al.[11]
(34) Kawanishi, Y.; Kitamura, N.; Tazuke, S. *Inorg. Chem.* **1989**, *28*, 2969.
(35) Rillema, D. P.; Allen, G.; Meyer, T. J.; Conrad, D. *Inorg. Chem.* **1983**, *22*, 1617.
(36) Kalyanasundaram, K. *Photochemistry of Polypyridine and Porphyrin Complexes*; Academic Press: London, 1992.
(37) Van Houten, J.; Watts, R. J. *J. Am. Chem. Soc.* **1975**, *97*, 3843.
(38) Caspar, J. V.; Sullivan, B. P.; Kober, E. M.; Meyer, T. J. *Chem. Phys. Lett.* **1982**, *91*, 91.
(39) Chen, P.; Meyer, T. J. *Chem. Rev.* **1998**, *98*, 1439.
(40) *Raman Spectroscopy* (in Japanese); Hamaguchi, H., Hirakawa, A., Eds.; Gakkai-Shuppan Center: Tokyo, 1988.